

Resonant magnetopolaron effect in a high electron density quantum well in a tilted magnetic field

S. N. Klimin,^{*} V. M. Fomin,[†] and J. T. Devreese[‡]*Theoretische Fysica van de Vaste Stoffen (TFVS), Universiteit Antwerpen, B-2020 Antwerpen, Belgium*

(Received 22 January 2008; revised manuscript received 16 April 2008; published 12 May 2008)

The cyclotron resonance (CR) spectra are calculated for a high electron density GaAs/AlAs quantum well in a tilted magnetic field. The CR peaks are split due to (i) the resonant magnetopolaron effect and (ii) the anticrossing of the CR mode and the plasmon-phonon intersubband modes. The derived CR peak positions and amplitudes are in good agreement with experiment. It is shown that the experimental CR spectra find an adequate explanation within Fröhlich's polaron concept.

DOI: [10.1103/PhysRevB.77.205311](https://doi.org/10.1103/PhysRevB.77.205311)

PACS number(s): 78.30.Fs, 71.38.-k, 78.66.Fd

I. INTRODUCTION

The polaron concept suggested by Landau¹ and developed by Pekar² and Fröhlich³ finds an experimental evidence in transport and optical properties of polar crystals. A survey of the polaron effects can be found, e.g., in Refs. 4–9. One of the manifestations of the electron-longitudinal optical (LO)-phonon interaction is the resonant magnetopolaron effect,^{10–12} i.e., anticrossing of zero-phonon and one-phonon levels of the electron-phonon system in a magnetic field, when the cyclotron energy $\hbar\omega_c$ is close to the LO-phonon energy $\hbar\omega_{LO}$. The resonant magnetopolaron effect has been experimentally observed in bulk,^{12–15} in two-dimensional (2D) electron gas, and in quantum-well structures.^{16–20}

In polar quantum wells and heterostructures with sufficiently high electron density, many-body effects play a substantial role. First, the anticrossing position shifts from $\hbar\omega_{LO}$ to the transverse optical (TO)-phonon energy $\hbar\omega_{TO}$, which is in accordance with experimental observations.^{21,22} Second, the Fröhlich electron-phonon interaction in these structures is screened, so that the resonant splitting of the cyclotron resonance (CR) lines at the anticrossing position is reduced in magnitude with respect to that in low-density polaron systems.

As mentioned in Ref. 23, a controversy exists regarding the problem of Fröhlich interaction: whether or not it manifests itself in the CR for a quasi-2D electron gas. In the recent experimental data on the photoconductivity of $\text{In}_x\text{Al}_{1-x}\text{As}$ quantum-well structures, both dielectric effects due to the multilayered structure and effects of the coupling between the 2D electron gas and the LO phonons are observed.^{24,25} In the experiments^{26–28} on the infrared transmission of a GaAs/AlAs quantum-well structure in a tilted magnetic field, two splittings of CR lines have been observed. One splitting is interpreted²⁷ in terms of anticrossing between the CR mode and the plasmon-phonon intersubband (PPI) mode by using a phenomenological model dielectric function of an electron gas in a quantum well. As indicated in Ref. 27, there is another splitting around the TO frequency, which is attributed in Ref. 27 to a possible interaction driven by the deformation potential.

The multidielectric model of the optical response for a quantum well^{27–29} is capable to explain some experimentally observed features of the magnetotransmission spectra of

high-density GaAs quantum wells without the explicit use of the electron-phonon interaction. In Refs. 28 and 29, a phenomenological relaxation time is introduced, which is used as a fitting parameter. In the present work, we consider a realistic electron-phonon interaction rather than a phenomenological relaxation time. The resonant splitting of the CR lines near $\hbar\omega_{TO}$ cannot be quantitatively interpreted by using the relaxation time as a fitting parameter. Below, we show that a quantum-mechanical study including both the electron-phonon interaction and the dielectric effects allows for the interpretation of the experimental CR spectra.^{26–28} In Refs. 30 and 31, the CR spectra in high-density GaAs quantum wells for a perpendicular magnetic field are interpreted in terms of magnetoplasmon-phonon mixing, which leads to a renormalization of polar optical phonons of a quantum well. It was shown in Refs. 30 and 31 that the approach beyond the model,²⁷ which takes into account the Fröhlich interaction, explains the splitting of the CR lines near $\hbar\omega_{TO}$ in high electron density quantum wells. In this connection, the polaron concept remains valid for doped quantum wells.

In the present paper, the approach of Refs. 30 and 31 is extended to the case of a tilted magnetic field. We calculate the absolute transmission of a quantum-well structure which contains an interacting polaron gas. The electron-phonon and electron-electron interactions are considered in terms of the memory function tensor (see Refs. 30, 32, and 33), taking into account their renormalization due to magnetoplasmon-phonon mixing.

The goal of the present work is to investigate the CR of an electron gas in a quantum well in the presence of a tilted magnetic field taking into account both the electron-phonon interaction and the dielectric effects. We show that the polaron effect is necessary for an adequate interpretation of the observed CR spectra in doped GaAs quantum-well structures in a tilted magnetic field. An accurate treatment of the polaron effect is also important in order to determine the band-edge effective mass.^{14,34} In Refs. 27 and 28, the cyclotron effective mass is a fitting parameter, so that the polaron correction is implicitly included into this effective mass. In the present investigation, similar to Ref. 30, where a quantum well in a perpendicular magnetic field was analyzed, the polaron correction to the electron band mass is explicitly calculated.

For a single magnetopolaron in a parabolic quantum well in the presence of a tilted magnetic field, the energy levels

and the polaron cyclotron mass have been calculated by using second-order perturbation theory.^{35,36} The magneto-plasma excitations for a parabolic quantum well in a tilted magnetic field have been theoretically studied within different approaches.^{37–39} The magnetoabsorption of an electron gas in a quantum well in a tilted magnetic field without the electron-phonon interaction has been considered, e.g., in Refs. 40–42. To the best of our knowledge, the resonant magnetopolaron effect for an interacting many-polaron system in a quantum well in the presence of a tilted magnetic field has not yet been investigated.

The paper is organized as follows. Section II represents the theoretical method for the analysis of the CR spectra of a high electron density quantum well in a tilted magnetic field. In Sec. III, the calculated transmission spectra are discussed and compared to experiment. Section IV contains conclusions.

II. OPTICAL RESPONSE OF A POLARON GAS IN A QUANTUM WELL IN A TILTED MAGNETIC FIELD

To describe an interacting polaron gas in a quantum well in the presence of a tilted magnetic field, we use a model parabolic confinement potential along the z axis, which allows one to analytically express the electron eigenstates.⁴³ In order to compare the theory to experimental data for a rectangular quantum well, the confinement frequency Ω_0 is chosen equal to the frequency of a transition between the ground and first excited size-quantized levels of the quantum well.

The Hamiltonian of an electron-phonon system in a quantum well within the effective-mass approach is

$$H = \sum_{\sigma} \int \psi_{\sigma}^{\dagger}(\mathbf{r}) \left[\frac{1}{2m_b} \left(-i\hbar \nabla + \frac{e}{c} \mathbf{A} \right)^2 + \frac{m_b \Omega_0^2}{2} z^2 \right] \psi_{\sigma}(\mathbf{r}) d^3r + \frac{1}{2V} \sum_{\mathbf{q}} \frac{4\pi e^2}{q^2 \epsilon_{\infty}} \mathcal{N}(\rho_{\mathbf{q}} \rho_{-\mathbf{q}}) + \sum_{\mathbf{q}} \hbar \omega_{\text{LO}} \left(b_{\mathbf{q}}^{\dagger} b_{\mathbf{q}} + \frac{1}{2} \right) + \frac{1}{\sqrt{V}} \sum_{\mathbf{q}} (V_{\mathbf{q}} b_{\mathbf{q}} \rho_{\mathbf{q}} + V_{\mathbf{q}}^* b_{\mathbf{q}}^{\dagger} \rho_{-\mathbf{q}}), \quad (1)$$

where m_b is the electron band mass, $\mathbf{A} = [0, B(x \cos \theta - z \sin \theta), 0]$ is the vector potential of a tilted magnetic field with the induction B and the tilt angle θ , ϵ_{∞} is the optical dielectric constant, $\psi_{\sigma}(\mathbf{r})$ [$\psi_{\sigma}^{\dagger}(\mathbf{r})$] is the annihilation (creation) operator for electrons, $b_{\mathbf{q}}(b_{\mathbf{q}}^{\dagger})$ is the annihilation (creation) operator for LO phonons with the frequency ω_{LO} , $\rho_{\mathbf{q}}$ is the density operator,

$$\rho_{\mathbf{q}} = \sum_{\sigma} \int e^{i\mathbf{q}\cdot\mathbf{r}} \psi_{\sigma}^{\dagger}(\mathbf{r}) \psi_{\sigma}(\mathbf{r}) d^3r, \quad (2)$$

$\mathcal{N}(\dots)$ is the symbol of a normal product of operators, $V_{\mathbf{q}}$ is the amplitude of the electron-phonon interaction, and V is the volume of a crystal. In Hamiltonian (1), we use the bulk LO phonons, which is consistent with the parabolic confinement potential.

The optical response of an interacting polaron gas in a quantum well is described by the optical conductivity tensor

$$\sigma_{jk}(\omega) = \frac{ie^2 n_S \omega}{m_b} [\mathcal{Q}^{-1}(\omega)]_{jk}, \quad (3)$$

with the 2D electron density, n_S , and the dynamic tensor of the system,

$$\mathcal{Q}(\omega) = \begin{pmatrix} \omega^2 - \Omega_0^2 \sin^2 \theta - \chi_{11}(\omega) & i\omega\omega_c - \chi_{12}(\omega) & \Omega_0^2 \sin \theta \cos \theta - \chi_{13}(\omega) \\ -i\omega\omega_c - \chi_{21}(\omega) & \omega^2 - \chi_{22}(\omega) & -\chi_{23}(\omega) \\ \Omega_0^2 \sin \theta \cos \theta - \chi_{31}(\omega) & -\chi_{32}(\omega) & \omega^2 - \Omega_0^2 \cos^2 \theta - \chi_{33}(\omega) \end{pmatrix}. \quad (4)$$

The effects of the electron-phonon and electron-electron interactions are taken into account through the memory function tensor $\chi_{jk}(\omega)$ (cf. Refs. 30, 32, and 33),

$$\chi_{jk}(\omega) = - \sum_{\mathbf{q}} \frac{|V_{\mathbf{q}}|^2 q_j q_k}{N \pi \hbar m_b \epsilon^2(\mathbf{q})} \int_{-\infty}^{\infty} d\omega' \{ D(\mathbf{q}, \omega') [G(\mathbf{q}, \omega - \omega') - G(\mathbf{q}, -\omega')] + D^*(\mathbf{q}, \omega') [G^*(\mathbf{q}, -\omega - \omega') - G^*(\mathbf{q}, -\omega')] \}. \quad (5)$$

Here, $\epsilon(\mathbf{q})$ is the static screening factor,³² and $G(\mathbf{q}, \omega)$ and $D(\mathbf{q}, \omega)$ are, respectively, the density-density electron Green's function and the phonon Green's function. The density-density electron Green's function is

$$G(\mathbf{q}, \omega) = -i \int_0^{\infty} e^{i\omega t - \delta t} \langle \rho_{\mathbf{q}}(t) \rho_{-\mathbf{q}}(0) \rangle dt, \quad \delta \rightarrow +0, \quad (6)$$

where $\langle \dots \rangle$ is the quantum-statistical average with the statistical operator of interacting electrons in a quantum well. The phonon Green's function is

$$D(\mathbf{q}, \omega) = -i \int_0^{\infty} e^{i\omega t - \delta t} [\langle b_{\mathbf{q}}(t) b_{\mathbf{q}}^{\dagger}(0) \rangle + \langle b_{-\mathbf{q}}^{\dagger}(t) b_{-\mathbf{q}}(0) \rangle] dt, \quad \delta \rightarrow +0. \quad (7)$$

Functions (6) and (7) are expressed in terms of the corresponding retarded Green's functions $G^R(\mathbf{q}, \omega)$ and $D^R(\mathbf{q}, \omega)$, as described in Ref. 30.

When taking into account the electron-phonon and electron-electron interactions, the phonon Green's function

for a quantum well describes the magnetoplasmon-phonon excitations^{44,45} rather than bare phonons. In the present work, we calculate the Green's functions in the random-phase approximation (RPA). The electron and phonon Green's functions are determined in the similar way as in Ref. 30. Within the approximation of a strong confinement, the phonon Green's function depend only on the tangential component \mathbf{q}_{\parallel} of the phonon wave vector. The retarded phonon Green's function within RPA is

$$D^R(\mathbf{q}_{\parallel}, \omega) = \frac{2[\omega_{\text{LO}} + \Pi(\mathbf{q}_{\parallel}, \omega)]}{(\omega + i\delta)^2 - \omega_{\text{LO}}^2 - 2\omega_{\text{LO}}\Pi(\mathbf{q}_{\parallel}, \omega)}, \quad \delta \rightarrow +0, \quad (8)$$

with the polarization operator

$$\Pi(\mathbf{q}_{\parallel}, \omega) = \sum_{q_z} \frac{|V_{\mathbf{q}}|^2}{\hbar^2 V} G^R(\mathbf{q}, \omega), \quad (9)$$

where $G^R(\mathbf{q}, \omega)$ is the retarded density-density electron Green's function. The phonon retarded Green's function is modified with respect to the bare-phonon retarded Green's function due to the electron-phonon interaction through the polarization operator $\Pi(\mathbf{q}_{\parallel}, \omega)$, which is provided by the electron-phonon interaction. The poles of the phonon retarded Green's function $\omega_s(\mathbf{q}_{\parallel})$ (where the index s numbers different magnetoplasmon-phonon branches) are numerically calculated as the roots of the equation,

$$\omega^2 - \omega_{\text{LO}}^2 - 2\omega_{\text{LO}} \text{Re} \Pi(\mathbf{q}_{\parallel}, \omega) = 0, \quad (10)$$

and correspond to the eigenfrequencies of the mixed magnetoplasmon-phonon modes of a quantum well. By using the Kramers–Kronig relation for $D(\mathbf{q}_{\parallel}, \omega)$, we find the Green's function, which enters the memory function,

$$D(\mathbf{q}_{\parallel}, \omega) = \sum_s \frac{A_s(\mathbf{q}_{\parallel})}{\omega - \omega_s(\mathbf{q}_{\parallel}) + i\delta} \quad [\omega_s(\mathbf{q}_{\parallel}) > 0, \delta \rightarrow +0], \quad (11)$$

where the coefficients $A_s(\mathbf{q}_{\parallel})$ are the residues of expression (8) at the points $\omega = \omega_s(\mathbf{q}_{\parallel})$.

In Refs. 22 and 26–28, the CR spectra are measured for the optical transmission of a GaAs quantum-well structure. In order to calculate the optical transmission of the structure in a tilted configuration, the total tensor dielectric function of a medium $\varepsilon_{jk}(\omega)$ is needed. This tensor is a sum of two terms, the dielectric function of the lattice, and the polaron contribution,

$$\varepsilon_{jk}(\omega) = \delta_{jk}\varepsilon_L(\omega) + \frac{4\pi i}{\omega} \sigma_{jk}(\omega), \quad (12)$$

where $\varepsilon_L(\omega)$ is given by

$$\varepsilon_L(\omega) = \varepsilon_{\infty} \frac{\omega^2 - \omega_{\text{LO}}^2}{\omega^2 - \omega_{\text{TO}}^2}, \quad (13)$$

with the TO-phonon frequency ω_{TO} , and $\sigma_{jk}(\omega)$ is the optical conductivity of an interacting polaron gas [Eq. (3)]. The transmission spectra of the quantum-well structure are then

calculated by using a set of electrodynamic boundary conditions for the electric and magnetic fields (cf. Ref. 28).

III. RESULTS AND DISCUSSION

In the numerical calculation, we use the material parameters for GaAs from Ref. 30: $\hbar\omega_{\text{LO}}=36.3$ meV, $\hbar\omega_{\text{TO}}=33.6$ meV, and $m_b=0.0653m_e$, where m_e is the free electron mass, $\varepsilon_{\infty}=10.89$, and $\alpha=0.068$. For an accurate determination of the CR energies, it is necessary to take into account the nonparabolicity of the conduction band. In the present paper, the memory function tensor [Eq. (5)] is calculated within the local parabolic band approximation.⁴⁶ The value 0.915 eV (Ref. 33) is used for the AlAs/GaAs potential barrier. For the energy levels in a nonparabolic conduction band, the formula from Refs. 46 and 47,

$$E_{nm} = \frac{E_0^*}{2} \left(\sqrt{1 + 4 \frac{E_{nm}^0}{E_0^*}} - 1 \right), \quad (14)$$

is applied with the effective energy gap $E_0^*=0.98$ eV (Ref. 47) and with the energy levels for a parabolic band,

$$E_{nm}^0 = \hbar\omega_1 \left(n + \frac{1}{2} \right) + \hbar\omega_2 \left(m + \frac{1}{2} \right), \quad (15)$$

where ω_1 and ω_2 are the eigenfrequencies of the electron states in a parabolic quantum well in the presence of a tilted magnetic field from Ref. 43.

A. Magnetoplasmon-phonon modes

Under the conditions of the CR ($\omega \sim \omega_c$), the dominant contribution to $\chi_{jk}(\omega)$ is provided by two branches of magnetoplasmon-phonon modes. In the case when both the electron-phonon interaction and the electron-electron interaction are neglected, these two branches correspond to the CR mode with the frequency ω_c and to the LO-phonon modes with the frequency ω_{LO} . When the electron-phonon interaction is taken into account, and the electron density is sufficiently high, an anticrossing of CR and LO-phonon modes occurs. The importance of the electron-electron interaction for the interpretation of the cyclotron resonance can be estimated using the plasma frequency,

$$\omega_p = \left(\frac{4\pi e^2 n_0}{m_b \varepsilon_{\infty}} \right)^{1/2}, \quad (16)$$

where $n_0=n_S/d$ is the three-dimensional electron density, d is the width of a quantum well. For a GaAs quantum well with $d=13$ nm and $n_S=7 \times 10^{11}$ cm⁻², the energy of a plasmon $\hbar\omega_p \approx 32.3$ meV is of the same order as the optical-phonon energies and, therefore, the electron-electron interaction is not negligible.

For a GaAs/AlAs quantum-well structure investigated in Ref. 27 (the sample with the electron density $n_S=7 \times 10^{11}$ cm⁻²), the frequencies $\omega_s(\mathbf{q}_{\parallel})$ and the coupling strengths $A_s(\mathbf{q}_{\parallel})$ for mixed magnetoplasmon-phonon modes are plotted in Fig. 1 as a function of the cyclotron frequency for several values of $q=|\mathbf{q}_{\parallel}|$ measured in units of $(m_b\omega_{\text{LO}}/\hbar)^{1/2}$.

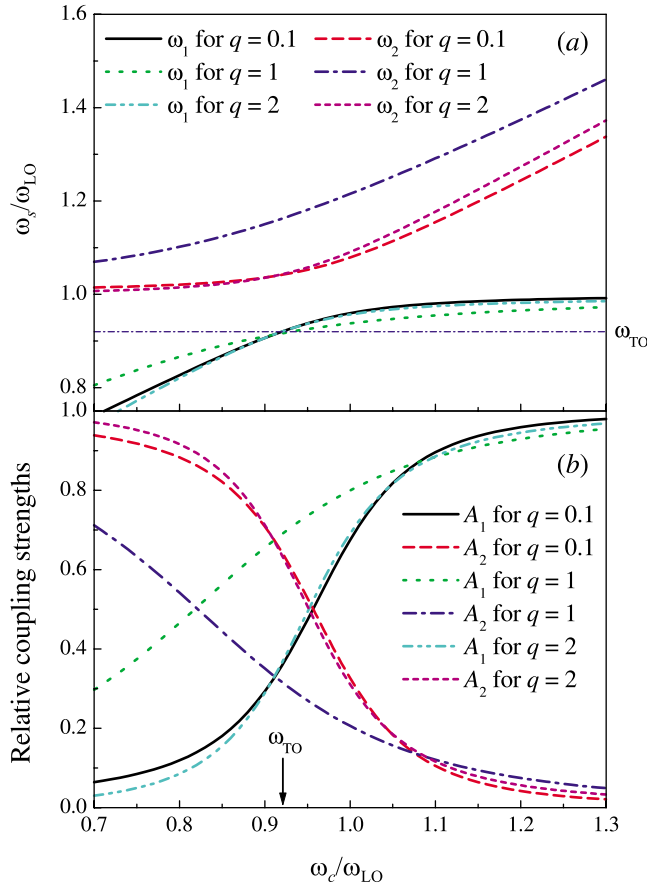


FIG. 1. (Color online) (a) Frequencies of the magnetoplasmon-phonon modes ($s=1$ for the lower-frequency mode and $s=2$ for the higher-frequency mode) for a 13 nm width GaAs quantum well with the electron density $n_s=7 \times 10^{11} \text{ cm}^{-2}$ as a function of ω_c in a perpendicular magnetic field for several values of $q=|q_{\parallel}|$. (b) Relative coupling strengths $A_s(\mathbf{q}_{\parallel})/\sum_s A_s(\mathbf{q}_{\parallel})$ of the magnetoplasmon-phonon modes corresponding to the frequencies shown in panel (a).

When $\omega_c \ll \omega_{LO}$, the frequency of one of the aforesaid magnetoplasmon-phonon branches is close to the frequency ω_c of the CR mode,²⁷ and the other frequency is close to ω_{LO} . In the case when the cyclotron frequency is of the same order as the optical-phonon frequencies, the anticrossing of CR and LO-phonon modes occurs [see Fig. 1(a)]. As a result of this anticrossing, the lower-frequency mode has the frequency close to ω_{TO} rather than to ω_{LO} when ω_c passes the region $\omega_c \sim \omega_{LO}$. In this region of values of ω_c , the lower-frequency mode dominates since $A_1(\mathbf{q}_{\parallel}) \gg A_2(\mathbf{q}_{\parallel})$ for $\omega_c \gtrsim \omega_{TO}$, as seen from Fig. 1(b). This behavior of frequencies $\omega_s(\mathbf{q}_{\parallel})$ and amplitudes $A_s(\mathbf{q}_{\parallel})$ explains the shift of the frequency of the resonant magnetopolaron effect in a high electron density quantum well from ω_{LO} to ω_{TO} . In this connection, the concept of the resonant magnetopolaron effect (cf. Ref. 28) as an anticrossing of the CR energies around the LO-phonon energy can be related only to the low-density case (according to our estimations, in GaAs quantum wells, the resonant magnetopolaron coupling occurs near ω_{LO} for $n_s \lesssim 10^{11} \text{ cm}^{-2}$). Other mechanisms (e.g., the deformation electron-TO-phonon interaction) can be hardly considered as a reason of the resonant coupling near ω_{TO} . As discussed in

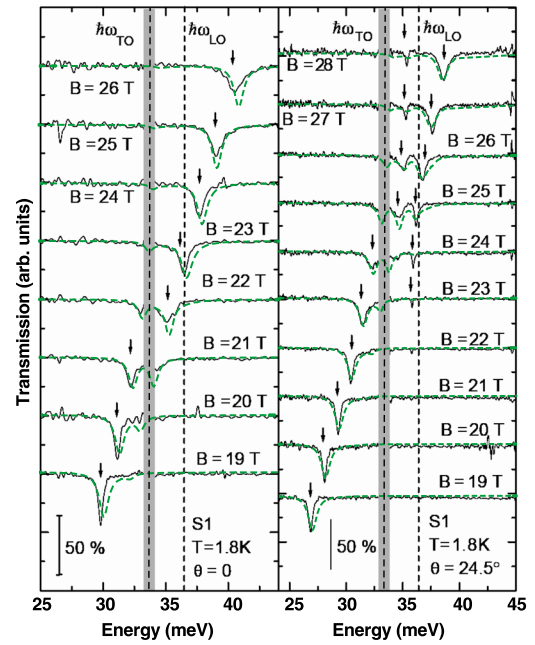


FIG. 2. (Color online) Relative transmission of a GaAs quantum-well structure in a perpendicular magnetic field (the left-hand panel) and in a tilted magnetic field (the right-hand panel) for different values of the magnetic field B . The experimental data (Ref. 26) are shown by solid black curves. The calculated CR spectra are plotted by dashed green curves.

Ref. 31, the anticrossing near ω_{TO} observed in Ref. 27 cannot be attributed to the deformation electron-phonon interaction because of symmetry reasons.

B. Cyclotron resonance spectra

In Refs. 26–28, the CR spectra are represented for the relative transmission,

$$T_R \equiv \frac{T_A}{T_A|_{B=0}}, \quad (17)$$

where T_A is the absolute transmission of a quantum-well structure. The relative transmission is considered instead of the absolute transmission in order to eliminate the contribution due to a strong optical absorption by TO phonons in the substrate. The absolute transmission of a quantum-well structure has been calculated by taking into account the full set of electromagnetic boundary conditions at the interfaces of the structure. In Fig. 2, we compare our theoretical relative transmission spectra with the experimental data of Ref. 26 for two values of the tilt angle: $\theta=0^\circ$ and $\theta=24.5^\circ$. As seen from Fig. 2, for both perpendicular and tilted configurations, there is a good agreement between our theory and experiment for all values of the magnetic field from the range selected in Ref. 26. Although the electron density in Ref. 26 is lower than that in the experiment of Ref. 22, the magnetoplasmon-phonon mixing is still substantial. As a result of this mixing, the CR spectra split at the frequency, which is close to the TO-phonon frequency. As distinct from the sample measured in Ref. 22, in the present case (when $n_s=7 \times 10^{11} \text{ cm}^{-2}$),

only the lowest Landau level is partly filled. Therefore, the splitting of the CR peaks due to the band nonparabolicity is absent. Nevertheless, the nonparabolicity influences the resonant frequency. For $\theta=24.5^\circ$ (the right-hand panel), the anticrossing of CR energies at $\omega \approx \omega_{\text{TO}}$ is manifested both in the calculated and measured CR spectra. An additional splitting of the CR peaks at $\hbar\omega \approx 35.62$ meV in a tilted magnetic field, which is discussed below, is also revealed in the calculated spectra.

In Fig. 3, we represent the cyclotron energies, which are determined from the peak positions of the calculated relative transmission spectra. The cyclotron energies are plotted as a function of the normal component of the magnetic field $B_n \equiv B \cos \theta$. The theoretical CR energies (solid curves) are superposed on the experimental data of Ref. 27 for different values of the tilt angle. As seen from Fig. 3, there is anticrossing of cyclotron energies in the range of the optical-phonon energies.

Figure 3(a) shows the calculated peak positions for the perpendicular configuration. The point, where the upper and lower branches of the cyclotron energies are at the closest distance from each other, is at about $B_n \approx 21$ T, with the CR energy close to the TO-phonon energy. The theoretical CR energies compare well with the experimental results. The experimentally observed splitting of the CR peaks, when the frequency of the incident light is close to ω_{TO} , finds an explanation in terms of the resonant magnetopolaron effect of electrons with mixed magnetoplasmon-phonon modes, in line with results of Ref. 30.

In Figs. 3(b) and 3(c), the comparison of our theory with the experiment²⁷ is performed for tilt angles other than zero. The experimental data represented in Fig. 2 of Ref. 27 demonstrate a double splitting of the CR spectra (near $\hbar\omega_{\text{TO}}$ and near $\hbar\omega \approx 35.62$ meV) for a tilted configuration. The splitting near ω_{TO} is due to the resonant magnetopolaron effect, as well as in the aforesaid case of a perpendicular magnetic field. The splitting at $\hbar\omega \approx 35.62$ meV results from a direct interaction of the mixed CR and PPI modes (see Refs. 48 and 49) with an incident light even without any account of the electron-phonon interaction. In the present treatment, we consistently take into account both the resonant magnetopolaron effect and the aforesaid mixing of CR and PPI modes. Therefore, our theory quantitatively explains all splittings observed in the experiment,²⁷ while the phenomenological approach of Refs. 27 and 28 does not predict any splitting near $\hbar\omega_{\text{TO}}$. As seen from Fig. 3, the theoretical CR energies are in good agreement with experiment for all values of the magnetic field and of the tilt angle taken in the measurements.

IV. CONCLUSIONS

We have investigated the cyclotron resonance of an interacting polaron gas in a GaAs quantum well by taking into account both the electron-phonon and electron-electron interactions. When the electron density is sufficiently high, the electron-phonon interaction is strongly influenced by screening and by the magnetoplasmon-phonon mixing. As a result of this mixing, a renormalization of LO-phonon modes oc-

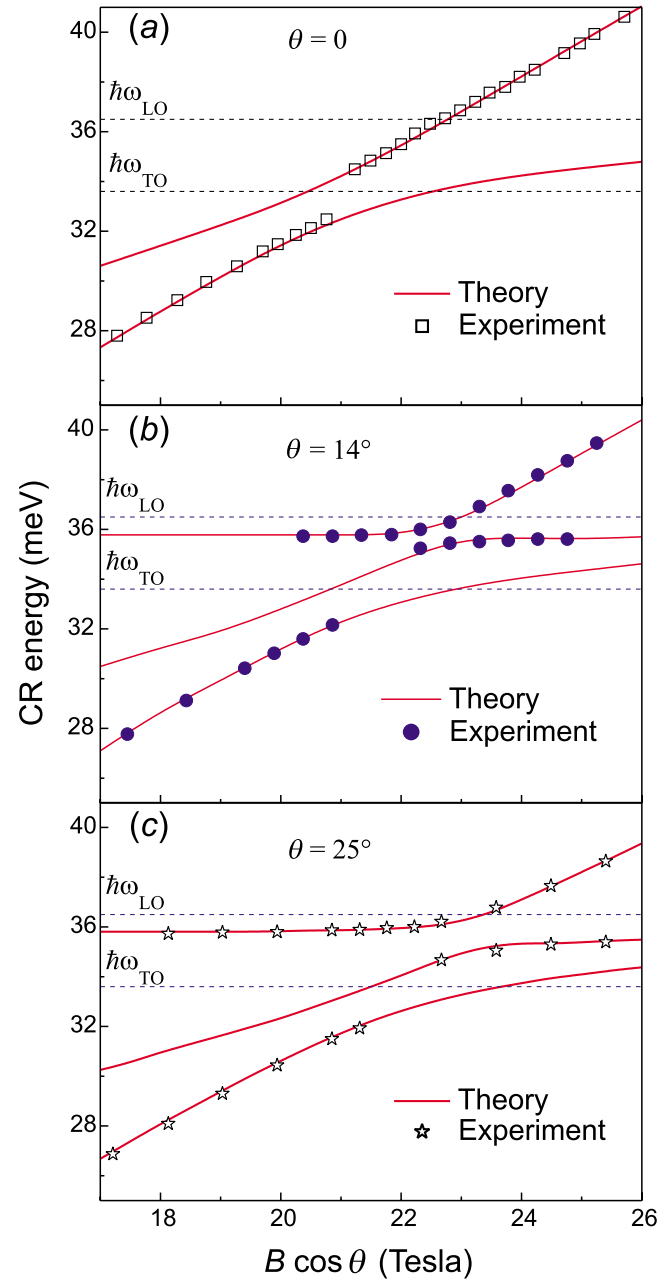


FIG. 3. (Color online) Experimental (Ref. 27) (symbols) and theoretical (curves) cyclotron energies for a 13 nm GaAs quantum well with the electron density $n_S = 7 \times 10^{11} \text{ cm}^{-2}$ in a tilted magnetic field at different values of the tilt angle θ . The dashed lines indicate LO- and TO-phonon energies. The theoretical cyclotron energies are determined by using the peak positions of the calculated CR spectra.

curs, so that the resonant magnetopolaron effect takes place for CR energies close to the TO-phonon energy in both perpendicular and tilted configurations of a magnetic field. For a tilted magnetic field, a double splitting of CR peaks occurs due to the resonant magnetopolaron effect and to the anticrossing of CR and PPI modes. The CR energies, obtained by using the well-established values for the conduction band parameters of GaAs, compare well with the experimental peak positions of Refs. 26–28.

The present work only partly resolves the problem brought to light in Refs. 27 and 28. In particular, the magnetopolaron effect—with the magnetoplasmon-phonon mixing—does not suffice to describe the observed shift of the resonant coupling energy from $\hbar\omega_{LO}$ to $\hbar\omega_{TO}$ in heterojunctions with relatively low carrier density $n_S \sim 3 \times 10^{11} \text{ cm}^{-2}$ (Ref. 50) without involving additional interaction mechanisms. However, the present investigation shows that the experimental data on CR for an electron gas in a polar quantum well, for sufficiently high carrier densities,²⁷ are in agree-

ment with a Fröhlich polaron description including many-body effects—screening and magnetoplasmon-phonon mixing.

ACKNOWLEDGMENTS

This work has been supported by the GOA BOF UA 2000, IUAP, and FWO-V Project Nos. G.0274.01N and G.0435.03, the WOG WO.035.04N (Belgium), and the European Commission SANDiE Network of Excellence, Contract No. NMP4-CT-2004-500101.

*On leave from Physics of Multilayer Structures, Department of Theoretical Physics, State University of Moldova, A. Mateevici 60, MD-2009 Chişinău, Moldova.

†Also at Photonics and Semiconductor Nanophysics, COBRA, Eindhoven University of Technology, P.O. Box 513, 5600 MB Eindhoven, The Netherlands. On leave from: Physics of Multilayer Structures, Department of Theoretical Physics, State University of Moldova, A. Mateevici 60, MD-2009 Chişinău, Moldova.

‡Also at Photonics and Semiconductor Nanophysics, COBRA, Eindhoven University of Technology, P.O. Box 513, 5600 MB Eindhoven, The Netherlands.

¹L. D. Landau, *Phys. Z. Sowjetunion* **3**, 664 (1933).

²S. I. Pekar, *Research on Electron Theory in Crystals* (Gostekhteorizdat, Moscow, 1951).

³H. Fröhlich, *Adv. Phys.* **3**, 325 (1954).

⁴*Polarons and Excitons*, edited by C. G. Kuper and G. D. Whitfield (Oliver and Boyd, Edinburgh, 1963).

⁵*Polarons in Ionic Crystals and Polar Semiconductors*, edited by J. T. Devreese (North-Holland, Amsterdam, 1972).

⁶*Polarons and Bipolarons*, edited by A. S. Alexandrov and N. Mott (World Scientific, Singapore, 1995).

⁷J. T. Devreese, *Encyclopedia of Applied Physics* (VCH, Weinheim, 1996), Vol. 14, p. 383.

⁸J. T. Devreese, *Encyclopedia of Physics*, edited by R. G. Lerner and G. L. Trigg (Wiley-VCH, Weinheim, 2005), Vol. 2, pp. 2004–2027.

⁹P. Calvani, *Optical Properties of Polarons* (Editrice Compositori, Bologna, 2001).

¹⁰D. Larsen, *Phys. Rev.* **135**, A419 (1964).

¹¹D. Larsen, in *Polarons in Ionic Crystals and Polar Semiconductors*, Ref. 5, pp. 237–287.

¹²E. J. Johnson and D. M. Larsen, *Phys. Rev. Lett.* **16**, 655 (1966).

¹³B. D. McCombe and R. Kaplan, *Phys. Rev. Lett.* **21**, 756 (1968).

¹⁴G. Lindemann, R. Lassnig, W. Seidenbusch, and E. Gornik, *Phys. Rev. B* **28**, 4693 (1983).

¹⁵P. Pfeffer, *Phys. Rev. B* **57**, 12156 (1998).

¹⁶Y.-H. Chang, B. D. McCombe, J.-M. Mercy, A. A. Reeder, J. Ralston, and G. A. Wicks, *Phys. Rev. Lett.* **61**, 1408 (1988).

¹⁷J. P. Cheng, B. D. McCombe, and G. Brozak, *Phys. Rev. B* **43**, 9324 (1991).

¹⁸F. M. Peeters, X. G. Wu, J. T. Devreese, C. J. G. M. Langerak, J. Singleton, D. J. Barnes, and R. J. Nicholas, *Phys. Rev. B* **45**,

4296 (1992).

¹⁹F. M. Peeters, X.-G. Wu, J. T. Devreese, M. Watts, R. J. Nicholas, D. F. Howell, L. van Bockstal, F. Herlach, C. J. G. M. Langerak, J. Singleton, and A. Chevy, *Surf. Sci.* **263**, 654 (1992).

²⁰Y. J. Wang, H. A. Nickel, B. D. McCombe, F. M. Peeters, J. M. Shi, G. Q. Hai, X.-G. Wu, T. J. Eustis, and W. Schaff, *Phys. Rev. Lett.* **79**, 3226 (1997).

²¹M. Ziesmann, D. Heitmann, and L. L. Chang, *Phys. Rev. B* **35**, 4541 (1987).

²²A. J. L. Poulter, J. Zeman, D. K. Maude, M. Potemski, G. Martinez, A. Riedel, R. Hey, and K. J. Friedland, *Phys. Rev. Lett.* **86**, 336 (2001).

²³A. Wyszomolek, D. Plantier, M. Potemski, T. Ślupski, and Ž. R. Zytewicz, *Phys. Rev. B* **74**, 165206 (2006).

²⁴K. Bittkau, N. Mecking, Y. S. Gui, Ch. Heyn, D. Heitmann, and C.-M. Hu, *Phys. Rev. B* **71**, 035337 (2005).

²⁵C. Faugeras, G. Martinez, F. Capotondi, G. Biasol, and L. Sorba, *Europhys. Lett.* **67**, 1031 (2004).

²⁶C. Faugeras, G. Martinez, A. Riedel, R. Hey, and K.-J. Friedland, *Physica E (Amsterdam)* **22**, 586 (2004).

²⁷C. Faugeras, G. Martinez, A. Riedel, R. Hey, K. J. Friedland, and Yu. Bychkov, *Phys. Rev. Lett.* **92**, 107403 (2004).

²⁸Yu. Bychkov, C. Faugeras, and G. Martinez, *Phys. Rev. B* **70**, 085306 (2004).

²⁹C. Faugeras, G. Martinez, A. Riedel, R. Hey, K. J. Friedland, and Yu. Bychkov, *Phys. Rev. B* **75**, 035334 (2007).

³⁰S. N. Klimin and J. T. Devreese, *Phys. Rev. B* **68**, 245303 (2003).

³¹S. N. Klimin and J. T. Devreese, *Phys. Rev. Lett.* **94**, 239701 (2005).

³²Xiaoguang Wu, F. M. Peeters, and J. T. Devreese, *Phys. Rev. B* **36**, 9760 (1987).

³³G. Q. Hai, F. M. Peeters, and J. T. Devreese, *Phys. Rev. B* **47**, 10358 (1993).

³⁴J. W. Hodby, G. P. Russell, F. M. Peeters, J. T. Devreese, and D. M. Larsen, *Phys. Rev. Lett.* **58**, 1471 (1987).

³⁵R. Haupt and L. Wendler, *Ann. Phys. (N.Y.)* **233**, 214 (1994).

³⁶G.-Q. Hai and F. M. Peeters, *Phys. Rev. B* **60**, 8984 (1999).

³⁷J. Dempsey and B. I. Halperin, *Phys. Rev. B* **45**, 1719 (1992).

³⁸E. Zaremba and H. C. Tso, *Phys. Rev. B* **49**, 8147 (1994).

³⁹D.-W. Wang, S. Das Sarma, E. Demler, and B. I. Halperin, *Phys. Rev. B* **66**, 195334 (2002).

- ⁴⁰L. Brey, N. F. Johnson, and B. I. Halperin, *Phys. Rev. B* **40**, 10647 (1989).
- ⁴¹A. Wixforth, M. Sundaram, J. H. English, and A. C. Gossard, *Surf. Sci.* **267**, 523 (1992).
- ⁴²J. Dempsey and B. I. Halperin, *Phys. Rev. B* **45**, 3902 (1992); **47**, 4662 (1993).
- ⁴³R. Merlin, *Solid State Commun.* **64**, 99 (1987).
- ⁴⁴L. Wendler and R. Pechstedt, *J. Phys.: Condens. Matter* **2**, 8881 (1990).
- ⁴⁵L. A. Falkovsky and E. G. Mishchenko, *JETP Lett.* **82**, 103 (2005).
- ⁴⁶X. Wu, F. M. Peeters, and J. T. Devreese, *Phys. Rev. B* **40**, 4090 (1989).
- ⁴⁷P. Pfeffer and W. Zawadzki, *Phys. Rev. B* **53**, 12813 (1996).
- ⁴⁸A. Pinczuk and J. M. Worlock, *Solid State Commun.* **36**, 43 (1980).
- ⁴⁹S. Holland, K. Bittkau, C.-M. Hu, Ch. Heyn, and D. Heitmann, *Phys. Rev. B* **66**, 233302 (2002).
- ⁵⁰R. J. Nicholas, L. C. Brunel, S. Huant, K. Karrai, J. C. Portal, M. A. Brummell, M. Razeghi, K. Y. Cheng, and A. Y. Cho, *Phys. Rev. Lett.* **55**, 883 (1985).